Applied Chemical Engineering (2026) Volume 9 Issue 3 ISSN: 2578-2010 (O)
doi: 10.59429/ace.v9i3.5997

RESEARCH ARTICLE

Determining the Dispersion Characteristics of a modified Venturi Using CFD and Validating them in a Flotation Column within a Water-Air-Mineral system

José Guadalupe González V[1], Ramiro Escudero García[1,*], Hugo Arcos Gutiérrez[2], Martín Reyes P[3]

[1] *Instituto de Investigación en Metalurgia y Materiales.Universidad Michoacana de San Nicolás de Hidalgo. Santiago Tapia 403. C.P.58000. Morelia, Michoacán, México*

[2] *CONAHCYT-CIATEQ, eje 126, No. 225, zona industrial, C.P. 78395, San Luis Potosí, S. L. P., México*

[3] *Área Académica de Ciencias de la Tierra y Materiales. Universidad Autónoma del Estado de Hidalgo. Mineral de la Reforma 42186. Pachuca, Hidalgo, México*

***Corresponding author:** Ramiro Escudero García, ramiro.escudero@umich.mx

ABSTRACT

The design, evaluation, and metallurgical validation of a modified Venturi-type gas disperser for controlling the dispersion characteristics (bubble diameter, retained gas volume, and bubble surface area) in a laboratory flotation column are presented. The design was carried out using CFD simulations in a transient regime, evaluating different geometric and air-supply configurations. The optimal configuration corresponds to a 3:1 diameter ratio and four air inlets at 45°, which generated stable pressure drops and homogeneous dispersion.

The simulated disperser was fabricated from polyamide and experimentally characterized in a water-air system under 35 operating conditions. Bubble diameters (Db) ranged from 0.63 to 2.31 mm, with retained gas fractions (εg) from 13 to 19% and bubble surface area flux (Sb) between 65 and 81 s^{-1}; these ranges are within the values typically recommended to improve particle capture and transport in column flotation.

The characteristics of the simulated and experimental dispersions show similarities with differences of less than 20%.

Subsequently, the disperser was evaluated in a three-phase system (water-air-mineral) for the concentration of a mineral containing 54 ppm of gold by reverse column flotation. The appropriate operating variables were established: superficial liquid velocity (Jl) of 0.0127 m/s, and superficial gas velocity (Jg) of 0.0085 m/s, achieving concentrations of up to 76 ppm Au in the tailings stream.

Experimental results demonstrate that controlling Db, εg, and Sb through CFD design and experimental validation directly affects the metallurgical performance of the process, establishing a comprehensive methodology for designing dispersers for mineral applications.

Keywords: CFD simulation, gas dispersions, column flotation, Venturi-type gas disperser, reverse flotation.

ARTICLE INFO

Received: 28 April 2026
Accepted: 10 June 2026
Available online: 21 August 2026

COPYRIGHT

Copyright © 2026 by author(s).
Applied Chemical Engineering is published by Arts and Science Press Pte. Ltd. This work is licensed under the Creative Commons Attribution-NonCommercial 4.0 International License (CC BY 4.0).
https://creativecommons.org/licenses/by/4.0/

1. Introduction

Column flotation is one of the most widely used technologies for separating mineral species of interest, particularly in the processing of fine minerals and in systems where selectivity is a critical factor [1,2]. The efficiency of the process depends largely on the bubble-particle interactions, which are governed by collision, adhesion, and detachment phenomena [1,3,4,5]. These phenomena are directly influenced by the system's dispersion characteristics, among which the bubble diameter (Db), the fraction of gas retained (ε_g), and the surface

flow of bubble area (Sb) stand out [1,2,6]. Several studies have indicated that bubbles in the approximate range of 0.5 to 2 mm and Sb values on the order of 100 s^{-1} increase the probability of capture and efficient transport of mineral particles, thereby improving the metallurgical performance of the process [6,7].

In industrial practice, precise control of gas-liquid dispersion characteristics presents a significant challenge. Many bubble generation systems operate empirically, with limited ability to manipulate bubble size or gas fraction to meet specific process needs [1,2]. In this context, Venturi-type dispersers constitute an attractive alternative due to their mechanical simplicity, low maintenance, and ability to induce air through pressure differentials generated by hydrodynamic effect; however, their performance depends on geometric parameters such as the ratio of diameters between the converging section and the throat, as well as the number and angle of the air inlets [8,9].

The development of simulation tools based on Computational Fluid Dynamics (CFD) has allowed progress in the rational design of hydraulic devices and multiphase systems [8,9].

CFD models simulate the hydrodynamic behavior of flotation systems by solving the incompressible Navier-Stokes equations. These models account for multiphase flow and turbulence, using approaches such as VOF (Volume of Fluid), LES (Large Eddy Simulation), and RANS (Reynolds Averaged Navier-Stokes). Among turbulence models, the k-ε (turbulent kinetic energy and dissipation model) stands out for estimating turbulent kinetic energy and its dissipation. These approaches make it possible to predict pressure distributions, local velocities, gas fraction, dispersion patterns, and bubble-particle behavior, which facilitates the analysis and optimization of Venturi dispersers and flotation systems without the need for extensive physical experimentation; however, the reliability of these models requires rigorous experimental validation when attempting to correlate dispersion variables with real metallurgical results [10].

CFD simulation of flotation columns or cells is scarce. In a two-phase air-water simulation of an FCMC cyclone flotation column using a CFD-PBM approach, researchers combined CFD with a population balance model to account for bubble size distribution. They represented turbulence using the k-ω SST model with curvature correction. The authors compared interfacial force models and selected a combination consisting of the Ishii-Zuber drag model, the Hosokawa-Frank wall lubrication model, and the López de Bertodano turbulent dispersion model. The model predicts gas fractions less than 10%. [11,12]

In flotation systems, determining the average bubble diameter is difficult because the devices are not transparent; therefore, measurement and estimation methods have been proposed and used to characterize Db in gas-liquid systems. In transparent systems, visual/photographic techniques provide a direct reference [13–15]. In this sense, the integration of CFD, mathematical models, and photographic validation constitutes a robust strategy and tool for characterizing dispersion in two-phase air-water systems [8,9,14,15].

A significant portion of the literature focuses on hydrodynamic characterization or model validation, without clearly establishing the quantitative relationship between dispersion variables (Db, ε_g, Sb) and metallurgical performance in real three-phase (liquid-gas-solid) systems. This connection is critical in flotation, as the presence of solids can modify coalescence, directly affecting Db and ε_g [16–18].

In gold-bearing minerals with a predominantly siliceous matrix, the use of cationic collectors such as dodecylamine favors the flotation of quartz under alkaline conditions, allowing gold-bearing particles to remain in suspension and be recovered in the understream tailings during reverse flotation [1,2]. In such systems, excessive increases in the surface gas velocity (J_g) can induce turbulence and coalescence, increasing Db and reducing the specific surface area available for selective interaction and mass transport, thereby affecting the recovery and grade of the mineral of interest [6,7,19].

In this context, the present work aims to design, validate, and metallurgically evaluate a modified Venturi-type gas disperser for application in the reverse flotation of a gold ore. The design was carried out using CFD

simulations in transient regimes, evaluating geometric configurations and selecting the configuration that produces stable dispersion with ε_g, Db, and Sb within the recommended ranges [6-9].

Subsequently, the disperser was manufactured and installed in a laboratory-scale column, where it was characterized in the air-water system using an estimation model and photographic validation [14,15,20]. Finally, its performance was evaluated in a three-phase air-water-mineral system, correlating hydrodynamic variables with gold concentration determined by chemical analysis using atomic absorption spectroscopy, and was also validated by fire assay (cupellation) [16–18].

The central hypothesis of this study is that geometric control of the Venturi disperser, along with appropriate selection of the superficial liquid and gas velocities (J_l and J_g), enables regulation of Db, ε_g, and Sb within an optimal range that maximizes concentration efficiency in reverse flotation. This work provides a comprehensive methodology that links CFD design, hydrodynamic validation, and metallurgical response, with potential applicability to scale-up under hydrodynamic similarity [8,9,19].

2. Materials and methods

2.1. Mineral and Physicochemical Characterization

The mineral sample (~50 kg) was collected from three points within a deposit in the state of Michoacán, Mexico. The material was homogenized and subsequently pulverized to obtain a representative sample for characterization and flotation tests.

The mineral density was determined using the helium gas technique with a Micromeritics® AccuPyc 1330 device [21]. Five determinations were performed. The chemical characterization was performed using X-ray fluorescence (XRF, Bruker S8 Tiger), X-ray diffraction (XRD, Siemens, mod. 5000), and atomic absorption spectroscopy (AAS, Perkin Elmer, 3100).

Particle size was determined using an array of 8 Tyler series sieves. 500 grams of a representative sample of the head mineral were placed in the mechanical shaker for 30 minutes. After this, the mineral mass retained on each sieve was weighed to determine the percentage by mass of particles passing through that sieve.

The head mineral showed a D80 of 280 µm. After pulverization, a D80 of 72 µm was obtained, a suitable value, considering that particle sizes in the tens to hundreds of micrometers are commonly reported as relevant for flotation performance, depending on the ore and conditions [22].

2.2. Geometric design and CFD modeling of the Venturi disperser

The Venturi-type disperser was designed with three main sections: convergent, throat, and divergent, as shown in Figure 1. Different diameter ratios (d1/d2) and air inlet configurations were evaluated.

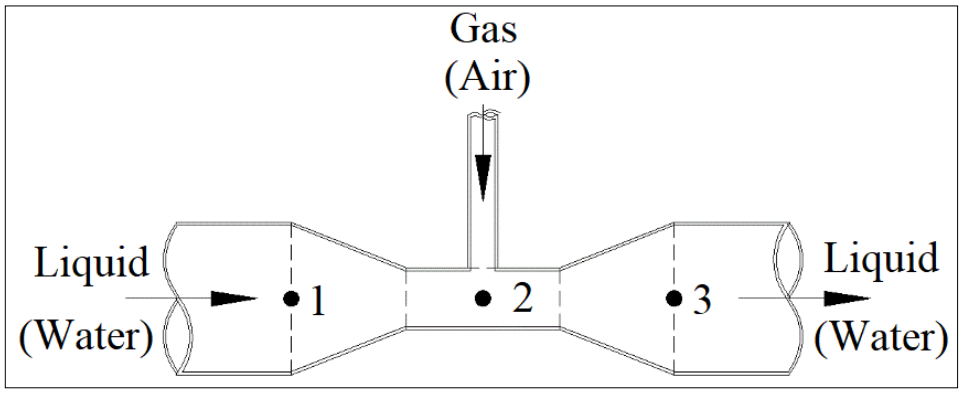


Figure 1. Schematic representation of a modified Venturi-type disperser; convergent diameter (d1), vena contracta or throat (d2), and divergent diameter (d3); (d3=d1).

2.2.1. Evaluated geometry

Five Venturi configurations were modeled, keeping the ratios of the convergent and divergent diameters (d1) and of the vena contracta (d2) constant, with d1/d2=3:1, and varying the number and angle of air supply inlets to the vena contracta.

Table 1. Dimensions of the Venturi simulated using CFD.

Venturi model	Venturi's largest diameter (m)	Venturi's smallest diameter (m)	Air phase inlets		
			Amount	Diameter (m)	Inlet angle
A	0.0381	0.0127	1	0.0064	90°
B	0.0381	0.0127	1	0.0064	45°
C	0.0381	0.0127	2	0.0064	45°
D	0.0381	0.0127	4	0.0064	45°
E	0.0381	0.0127	8	0.0064	45°

The simulated configurations: a 3:1 diameter ratio (converging and diverging diameters of 0.0381 m and a throat diameter of 0.0127 m); four air inlets with a diameter of 0.0064 m, in one simulation at 90° and four other simulations at 45° with respect to the flow axis. The geometry was created in AutoCAD® and exported in *.iges format for import into ANSYS®.

Finally, based on the simulation, the configuration with the highest and most stable pressure drop in the venturi was selected for the experiment with the venturi installed in the flotation column.

2.3. CFD Simulation

The simulations were performed in ANSYS Fluent® using a finite-volume transient scheme. A two-phase model (water as the primary phase and air as the secondary phase) and the standard k–ε turbulence model were used. The use of turbulence modeling (including k–ε formulations) is common in engineering simulations for turbulent and multiphase flows [10].

2.3.1. Border conditions

Water inlet conditions with a fixed flow rate, independent air inlets, a mixing outlet, and non-slip wall conditions were established. Initial simulations were performed for 10 s for geometric selection and subsequently extended to 60 s by coupling the Venturi to a flotation column with a 0.10 m diameter and a 2.60 m height. The monitored variables included differential pressure in two fixed points to calculate gas volume fraction in a certain portion of the column, and velocity fields [8,9].

2.3.2. Mesh design

Meshing is a fundamental stage of CFD simulation, as it divides the three-dimensional geometry of the Venturi diffuser into small control volumes. Variables such as pressure, velocity, and gas fraction are calculated for each element, enabling an approximation of the hydrodynamic behavior of the entire system. Meshing was performed using the ANSYS Fluent Meshing tool, adjusting the number of divisions per node, edge, surface, and volume. A fine mesh increases the accuracy of the results but also demands more computing resources; conversely, a coarse mesh reduces calculation time, although it increases the margin of error. Each of the five Venturi configurations was meshed independently, considering its specific geometric characteristics. The models with four and eight air inlets exhibited greater topological complexity. Additionally, during this stage, the surfaces that would later serve as the system's inlets, outlets, and walls were identified.

The steps involved in optimizing the venturi geometry can be summarized through the following flowchart.

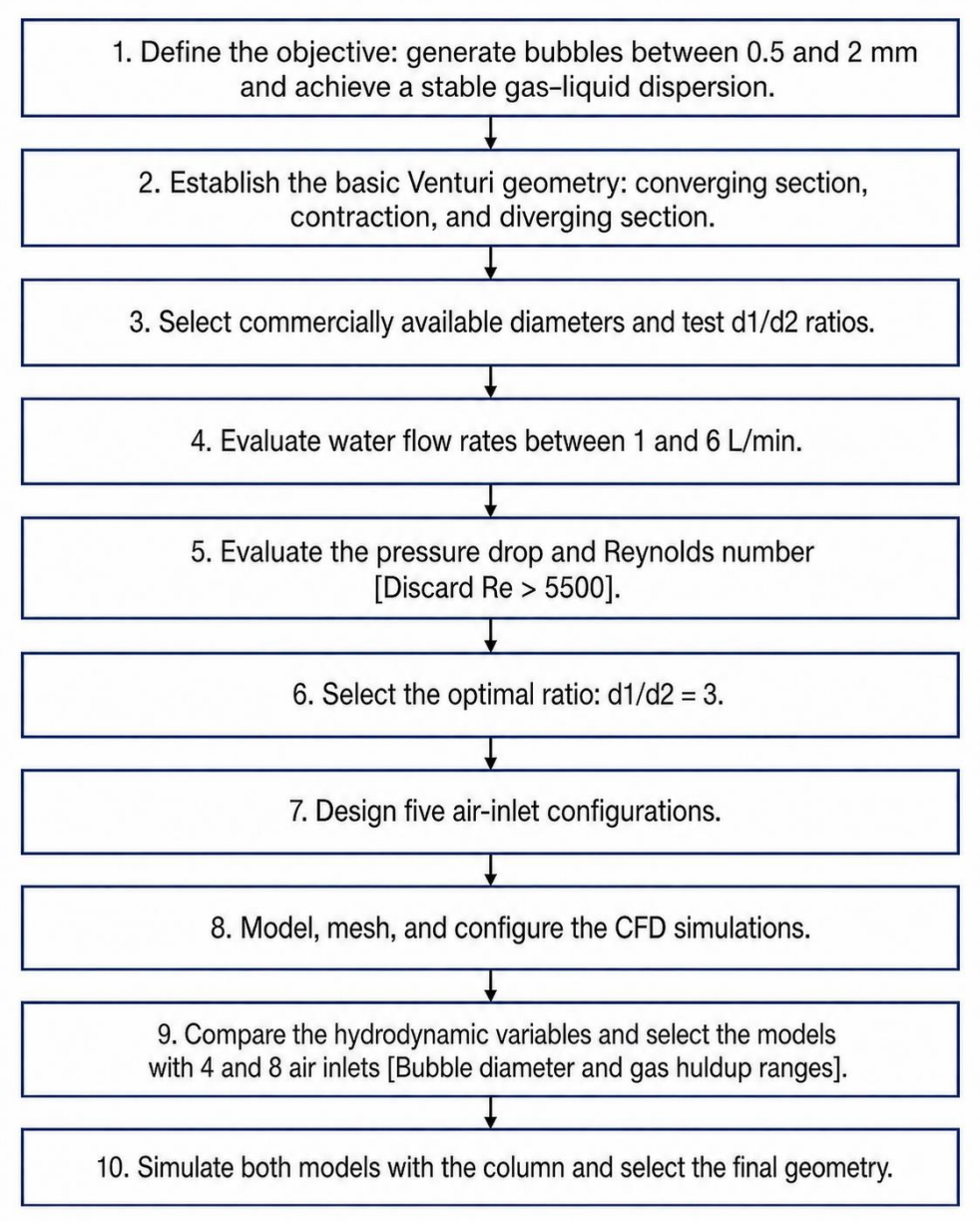


Figure 2. Flowchart to optimize the final geometry of the venturi.

2.4. Flotation column set-up

2.4.1. Two-phase experiments. Determination of bubble diameter.

A column of transparent acrylic material with a flat section at its top was manufactured to photograph bubble clouds and measure their diameters under different gas and liquid flow conditions. The bubble diameter was estimated using the Drift-Flux model supported by pressure and flow measurements, complemented by photographic analysis.

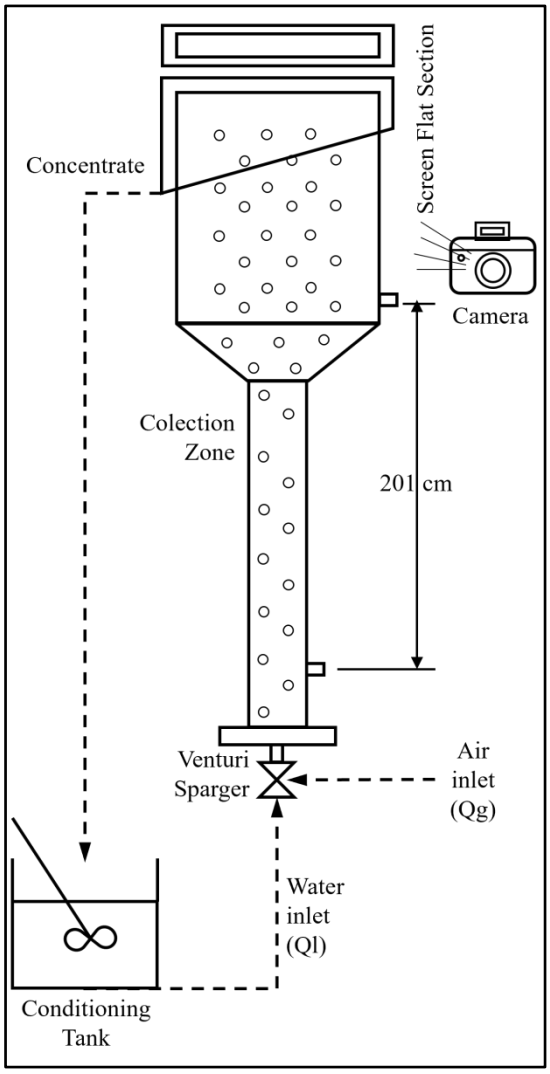


Figure 3. Experimental setup to obtain evidence of a bubble swarm through photographs to estimate the average Db. Air-water system.

Bubble diameter validation was performed using high-speed photographs taken under 35 different flow conditions. For each condition, a central area of 0.05 × 0.05 m was analyzed, and 300 bubbles were measured using AutoCAD®, resulting in approximately 10,500 bubbles evaluated per air and water flow combination. Based on statistical analysis of the measured bubbles, Db80 (80% of the bubbles with diameters smaller than the others) was determined as the representative diameter. The specific surface area of the bubble (Sb) was calculated as a function of εg and Db, in line with hydrodynamic definitions commonly used in column flotation [6,7,20].

2.4.2. Three-phase experiments. Reverse flotation.

The influence of solids on gas volume and coalescence is well documented in flotation columns and motivated the evaluation of the disperser in a three-phase system [16-18]. For reverse flotation experiments in the water-air-mineral system, a pulp was prepared with 10% by volume of ore (1.095 kg in 30 L of water), pH ranging from 10.5 to 11 by adding NaOH, dodecylamine as a cationic collector at concentrations of 1×10^{-4} and 1.5×10^{-4} Molar, and pine oil as a frother to fix the surface tension (σ) at 0.050 N/m +/- 0.1%. Liquid and gas flow rates (Ql and Qg) were varied, and the gold concentrations in the different streams were analyzed by AAS.

A cylindrical column made of transparent acrylic material, 2.60 m high and 0.10 m in internal diameter, was used. The system included a homogenization tank (30 L), a centrifugal feed pump, and a sphere rotameter at each air inlet point to the venturi. The level of the foam zone/collection zone interface (0.05 m from the top

of the column) was controlled by the flow in the tail stream. Once the system was stable, samples were collected from the feed streams, concentrate, and tailings.

The monitored variables were water and gas flow rates, along with pressure drop in a portion of the column, to estimate the gas volume fraction ε_g. The bubble diameter was estimated using a drift flux model, which uses the values of the monitored variables for its solution, as well as data on the physical and chemical properties of the phases present in the system [2, 6, 15, 16]. Two pressure sensors were installed 2.10 m apart. The signals were acquired and processed using a LabVIEW® routine. For each condition, 40 readings were recorded per sensor (500 ms; 20 s), and the average was used as the representative value. The gas retention fraction (ε_g) was determined from the pressure differential divided by the distance between the sensors.

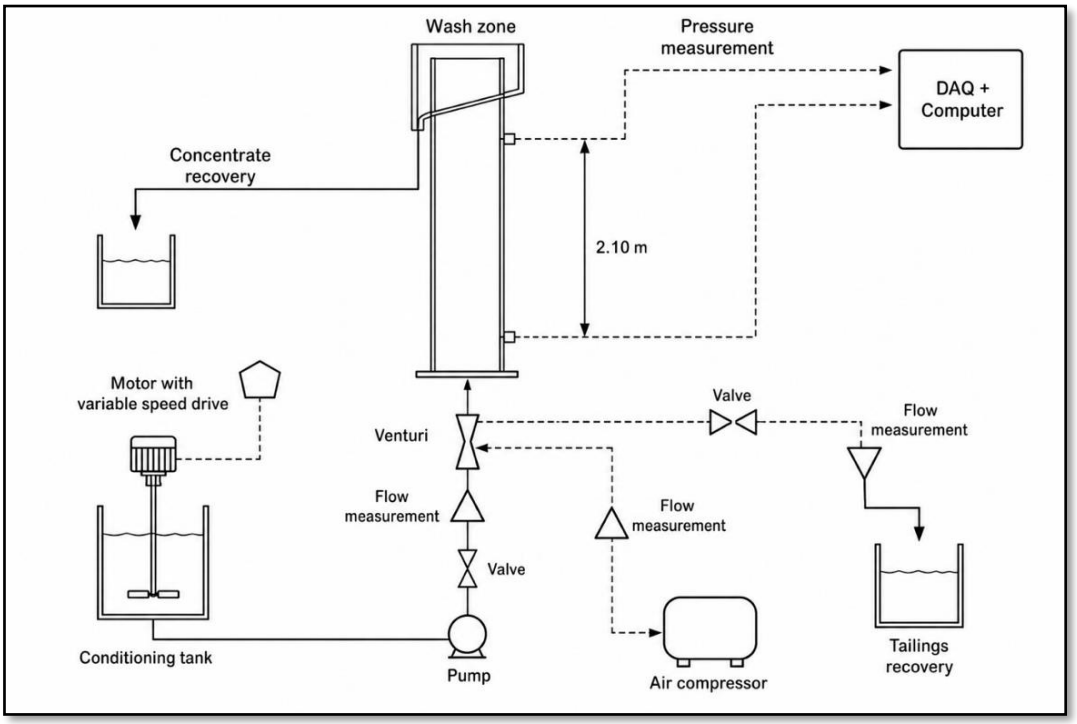


Figure 4. Experimental setup for the recovery of gold particles by reverse flotation.

3. Results

3.1. Geometric evaluation and selection of the disperser using CFD

The first stage consisted of evaluating Venturi-type disperser configurations using Computational Fluid Dynamics in a transient regime, recognizing that CFD provides a numerical framework for predicting the hydrodynamic behavior of gas-liquid systems by solving the continuity and Navier-Stokes equations within a discretized domain [8,9]. The Venturi geometry consists of three main regions: a converging section, a contraction (throat), and a diverging section. Different diameter ratios and air supply configurations were evaluated. Five diffuser designs were analyzed, varying mainly in the number and angle of the air inlets.

Figure 5 shows the simulation results of bubble generation with the Venturi-type disperser using the k-ε and LES turbulence models. The results were used to select the final Venturi design for the flotation column experiments.

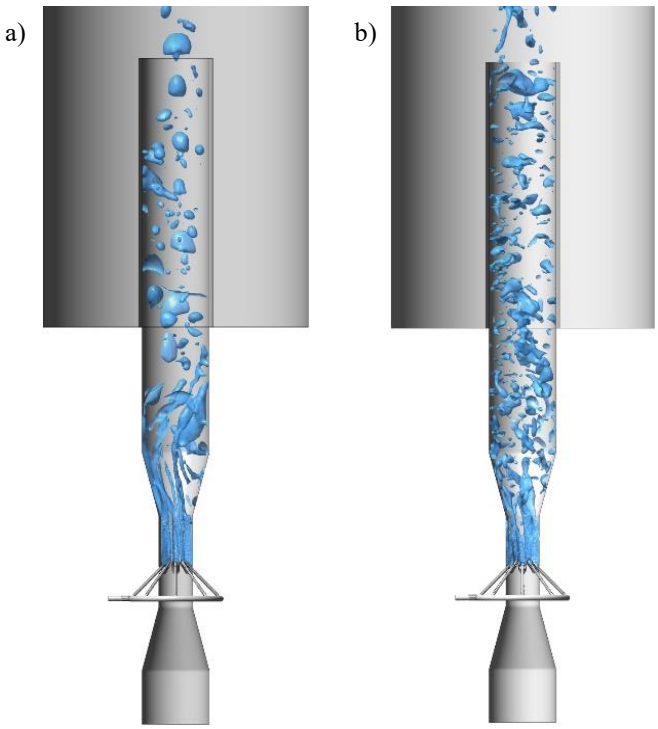


Figure 1. CFD image of the generation of bubbles with the venturi type disperser, a) simulation with k-ε; b) simulation with LES.

There is a difference between the simulation models in terms of dispersion and bubble size. The simulations made with the model k-ε have bubbles with a larger size (Figure 5a); this is caused by the phenomenon of coalescence, derived from the recirculation that occurs in the convergent area of the venturi; in addition, a great part of the flow of bubbles is channeled through a certain zone of the column. This fact will very likely cause some mixing.

In addition to the above results, the other selection criteria were pressure differential stability, gas retention (εg), and bubble generation within the recommended diameter range of 0.5 to 2 mm [6,7]. After initial simulations, configurations with four and eight air inlets were selected for more extensive simulations, including those of a laboratory-scale flotation column. These results, shown in Figures 6 and 7, supported the final selection of the Venturi geometry for construction and experimental validation.

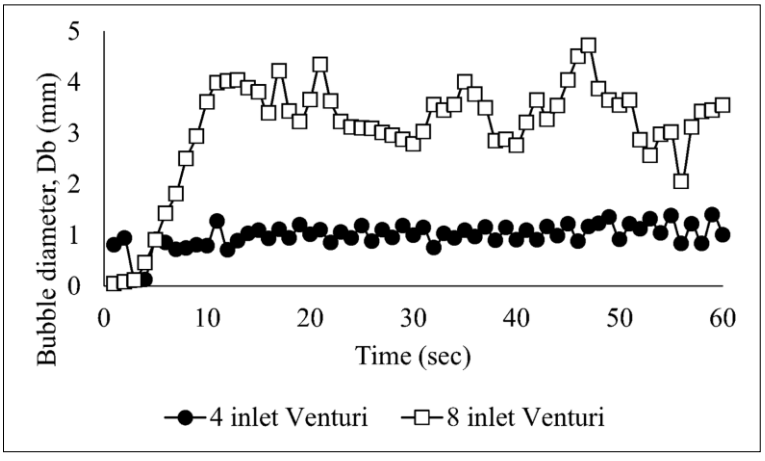


Figure 6. Bubble Diameter for Venturi with 4 and 8 air inlets, in simulation up to 60 seconds with column.

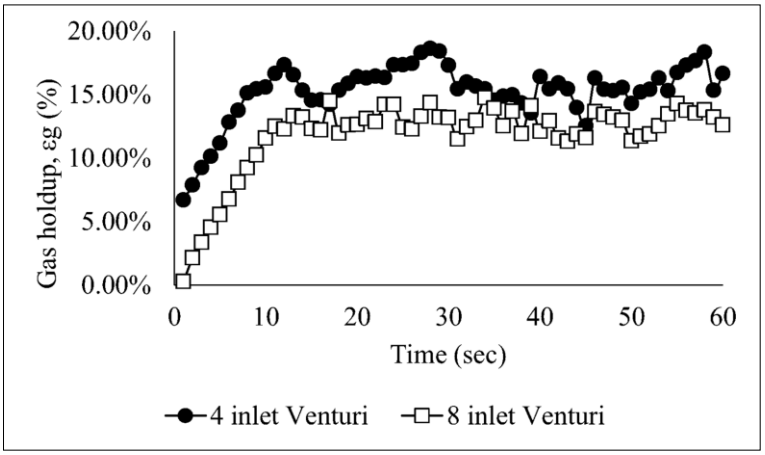


Figure 7. Gas fractions calculated from pressure drop values. Simulation up to 60 seconds of Venturi with 4 and 8 air inlets with a column.

By extending the simulation to 60 s and incorporating the entire column, the configuration with four inlets at 45° and a 3:1 ratio achieved a stable regime with ε_g 13–18% and bubbles in the desired range (0.5–2 mm); These values are consistent with reports relating dispersion (ε_g, Db, Sb) to performance in flotation columns[6,7]. In contrast, the Venturi with eight inlets exhibited greater size dispersion and lower ε_g stability. Conditions with Re > 5500 were ruled out, as excessive turbulence favors coalescence and increases the diameter of the bubbles. Based on these results, the final selection of the Venturi geometry for construction and experimental validation was 4 air inlets at 45 degrees with respect to the disperser's longest longitudinal axis, with a diameter ratio of 3:1.

3.2. Characteristics of dispersions in the water-air system using photographic techniques.

The disperser, constructed from Nylamid®, was characterized in a 0.10 m diameter column under 35 operating conditions. The diameters obtained by Drift Flux and validated photographically ranged from 0.63 to 2.31 mm. Figure 8 shows an example of the photographic evidence obtained to estimate the average bubble diameter under certain water and air flow conditions.

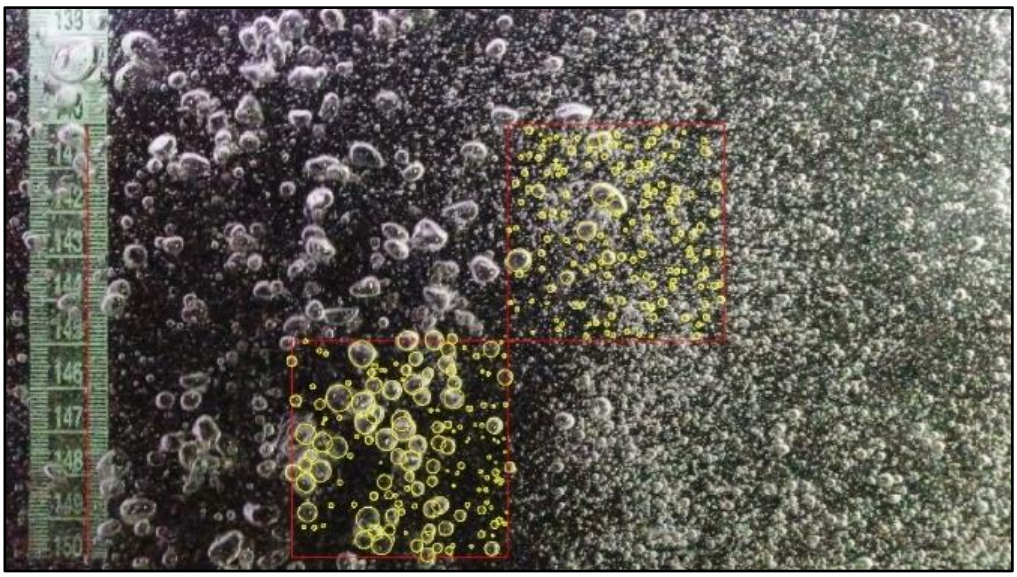


Figure 8. Example of bubble diameter measurement in the air-water system under specific air and water flow conditions. The tape inside is for calibrating the image analyzer.

On the other hand, Table 2 shows the Db values measured from photographic evidence and those calculated by solving the Drift Flux model using CFD simulation and experimental data.

Table 2. Comparison of measured Db_{80} (photographic technique) and Db calculated by simulation and estimated with Drift Flux from experimental data.

Water flowrate (Q_l), L/min	Air flowrate (Q_g), L/min	D_{b80}, mm		
		Photo	CFD	Drift Flux
4	4	0.88	0.83	0.75
	5	1.45	1.54	1.22
	6	1.42	1.33	1.1
	7	1.45	1.62	1.24
	8	1.44	1.38	1.18
	9	1.43	1.6	1.19
	10	1.43	1.27	1.23
5	4	0.92	1	0.91
	5	0.88	0.78	0.87
	6	0.9	1	0.93
	7	0.98	0.91	1.01
	8	0.95	0.97	1.03
	9	1.42	1.29	1.36
	10	1.47	1.66	1.42
6	4	0.92	0.88	0.99
	5	0.96	1.04	1.17
	6	0.92	0.88	1.1
	7	1.47	1.59	1.6
	8	1.44	1.3	1.6
6	9	1.44	1.5	1.33
	10	1.42	1.41	1.43
7	4	0.92	0.97	1.14
	5	1.47	1.31	1.7
	6	1.48	1.55	1.31
	7	1.46	1.39	1.37
	8	1.45	1.49	1.55
	9	1.42	1.38	1.25
	10	0.92	0.94	1.15
8	4	0.93	0.91	1.12
	5	0.94	1.03	1.12
	6	1.99	1.87	2.05
	7	1.46	1.61	1.79
	8	1.47	1.35	1.66
	9	1.44	1.56	1.56
	10	1.43	1.42	1.48

It was identified that J_g values close to 0.01 m/s favor more homogeneous bubbles and less dispersion in Db_{80}, consistent with dispersion characteristics reported for columns [6,7]. The gas fraction retained (ε_g) remained at 13–19 %, while Sb ranged from 65 to 81 s^{-1}, within ranges reported as favorable for efficient column flotation operation [6,7]. The analysis shows that increases in J_g raise ε_g; however, the increase in effective surface area is not proportional due to the growth of Db through turbulence-induced coalescence, a behavior expected in columns as gas flow increases [19].

3.3. Validation of bubble diameter from simulation and experimental techniques

Figure 9 compares the bubble diameters obtained using the three techniques (photographs, simulation, and experiment) with estimates from the drift-flux model, solved for the simulation and the experiment. The dashed lines represent an error of +/- 20%. The comparison between diameters shows differences generally less than 20%, confirming the consistency of the hydrodynamic characterization methods used in gas-liquid systems [14,15].

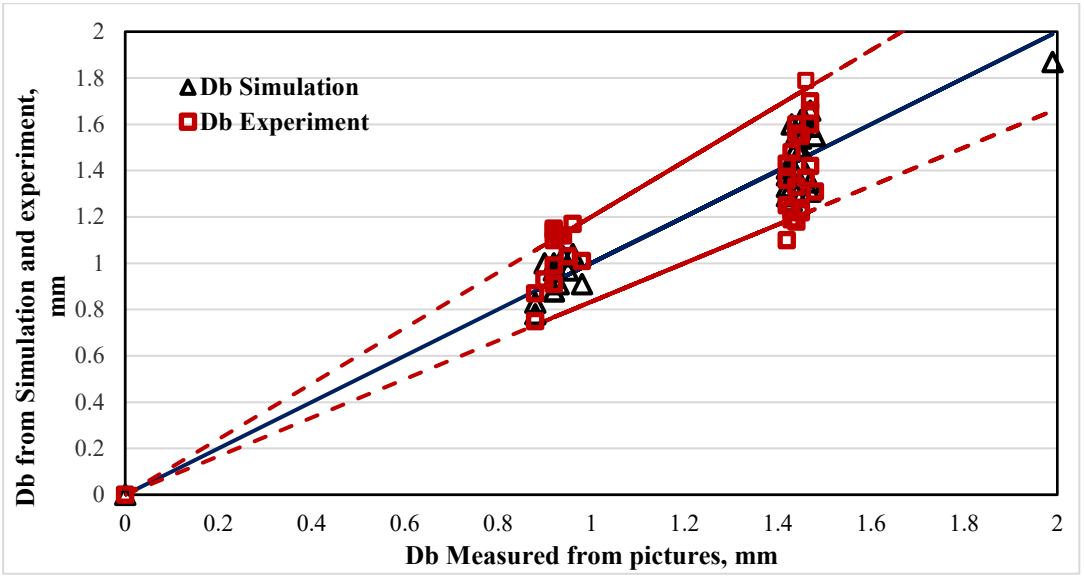


Figure 9. Comparison between the estimated and measured value of Db80. The dashed lines represent a margin of error of ±20% in this comparison.

The former figure presents all the measured and calculated Db results for the water and air flows included in this study, as well as for the geometric characteristics of the 4-inlet Venturi diffuser. In Figure 10, the data is presented differently; the area under this "sheet" represents the Db values that can be generated and controlled by various combinations of air and water flows through the venturi.

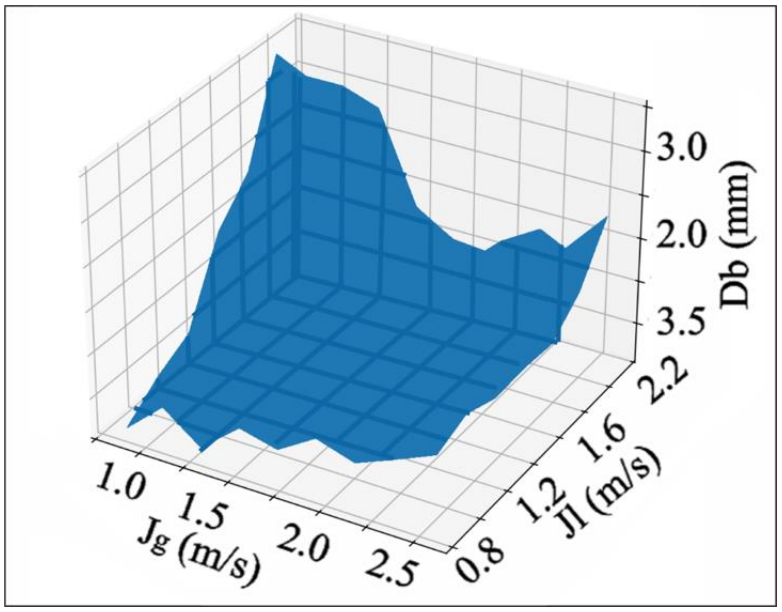


Figure 10. Bubble diameters generated by the Venturi in Nylamid for the water-air system in the 0.10 m diameter flotation column.

3.4. Gold concentration by reverse flotation in the 0.10 m diameter column.

The head mineral had an average Au concentration of 54 ppm. Table 3 shows the results of the chemical analysis by AAS of the tailings streams (rich in gold particles) and of the concentrate containing particles of no metallurgical interest. It can be seen that the maximum concentration (76 ppm) was obtained in the tailings stream samples, for J_l = 0.0127 m/s, J_g = 0.0085 m/s, and ε_g = 16.7%. By increasing J_g to 0.0212 m/s, the concentration decreased to 49 ppm. This behavior is due to bubble coalescence, which alters the Sb and bubble particle capture efficiency (or loading capacity). [6,7,19].

Table 3. Results of the chemical analysis by AAS on samples from the three streams during reverse flotation in the 0.10 m diameter column.

	EXPERIMENTS					
Exp. Number	1	2	3	4	5	6
Q_l (L/min)	4	6	4	4	4	8
Q_g (L/min)	4	4	6	8	10	4
J_l (m/s)	0.0085	0.0127	0.0085	0.0085	0.0085	0.0170
J_g (m/s)	0.0085	0.0085	0.0127	0.0170	0.0212	0.0085
ε_g (%)	14.9	16.7	16.5	17.1	19.1	13.2
Au in Tailings (ppm)	60	76	56	52	49	72
Au in Concentrate stream (ppm)	49	57	59	55	45	45
Residual Au in conditioning tank (ppm)	53	63	42	56	49	54

According to the table above, the gold in the concentrate stream refers to the Au contained in the stream that comes out of the top of the column, and which in this case of reverse flotation, contains the mineral species without metallurgical value.

Figures 11 and 12 show the relationship between gold concentrations and the appropriate operating conditions for maximum recovery. The flotation data were analyzed under six operating conditions, each performed in triplicate. For each condition, the average values of the gas fraction retained (εg) and the gold concentration in the tank, outlet, and tailings were calculated.

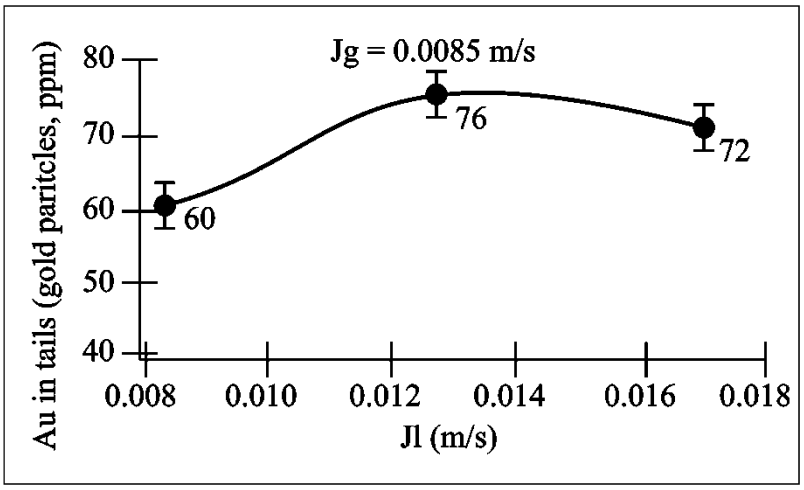


Figure 11. Concentration by flotation in a 0.10 m column. Operating conditions: J_g constant at 0.0085 m/s and J_l variable between 0.0085 and 0.017 m/s.

The behavior in Figure 11 indicates that, for the optimum J_g of 0.0085 m/s, there is a maximum feed flow of mineral pulp to the column of 0.0127 m/s, after which the gold recovery decreases by modifying the hydrodynamic behavior of the column.

On the other hand, Figure 12 clearly shows the effect of air overfeeding to the column through the venturi disperser, which causes bubble coalescence and a decrease in gold recovery in the tailings stream, as the non-valuable particles end up in the tailings stream.

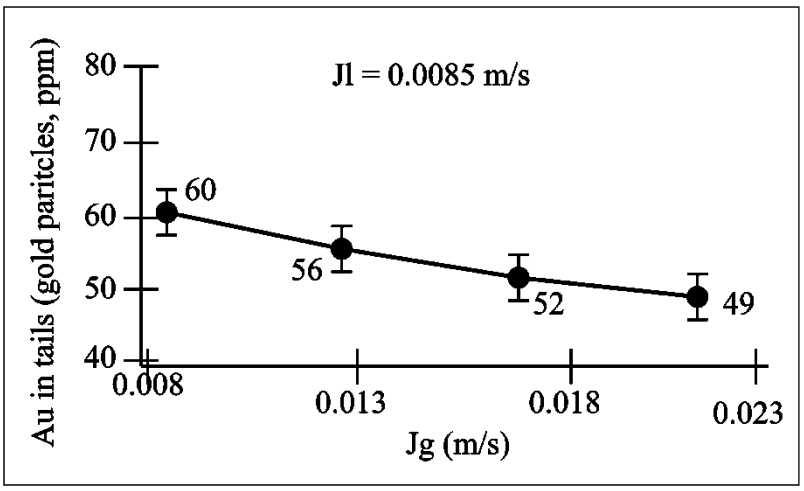


Figure 12. Reverse flotation in a 0.10 m column. Operating conditions: J_l constant at 0.0085 m/s and J_g variable between 0.0085 and 0.022 m/s.

4. Conclusions

- Comparing bubble diameters measured using photographic techniques with those calculated through the resolution of the Drift Flux model for CFD simulation data and experimental results demonstrates that simulation is a valuable tool for the design of Venturi-type gas dispersers for installation in gas dispersion systems, which, linked to metallurgical results, constitutes a comprehensive methodology for optimizing flotation processes.

- CFD simulation enables the selection of the optimal Venturi disperser geometry. In this case, a 3:1 ratio and four inlets at 45° are used, resulting in stable pressure drops and homogeneous gas dispersion.

- The modified venturi-type disperser allowed control of Db (0.63–2.31 mm), ε_g (13–19%), and Sb (65–81 s^{-1}), in ranges compatible with the dispersion characteristics reported for efficient column flotation.

Author contributions

José Guadalupe González: Investigation, Data curation, Formal analysis, Writing—original draft. Ramiro Escudero García: Investigation, Formal analysis, Writing—review & editing. Hugo Arcos Gutierrez: Conceptualization, Writing—review. Martín Reyes P.: Writing—review.

Acknowledgments

José Guadalupe González Valencia deeply thanks UMSNH for the support during his Ph.D. studies.

Conflict of interest

The authors declare no conflict of interest.

Data availability

The datasets generated during and/or analyzed during the current study are available from the corresponding author on reasonable request.

References

1. A. Gupta, D.S. Yan, Chapter 16 - Flotation, Editor(s): A. Gupta, D.S. Yan, Mineral Processing Design and Operation, Elsevier Science, 2006, Pages 555–603, ISBN 9780444516367. https://doi.org/10.1016/B978-044451636-7/50017-6
2. Dobby & Finch, 1990. Column Flotation, Pergamon Press.

3. Jameson, G. J., Nam, S., Moo-Young, M. (1977a). Physical factors affecting recovery rates in flotation. Min. Sci. Eng., 9(3), 103–118.
4. Yusheng Wang, Lisha Dong, Xiangning Bu, Chao Ni, Guangyuan Xie. Study on inhibition mechanisms of detachment of coal particles from oily bubbles in flotation column, Powder Technology, Volume 434, 2024, 119368, ISSN 0032-5910, https://doi.org/10.1016/j.powtec.2024.119368
5. Xiangning Bu, Shaoqi Zhou, Meng Sun, Muidh Alheshibri, Md. Shakhaoath Khan, Guangyuan Xie, and Saeed Chehreh Chelgani. Exploring the Relationships between Gas Dispersion Parameters and Differential Pressure Fluctuations in a Column Flotation. ACS Omega 2021, 6, 21900−21908. https://doi.org/10.1021/acsomega.1c01955
6. López-Saucedo, F., Uribe-Salas, A., Pérez-Garibay, R., & Magallanes-Hernández, L. (2012). Gas dispersion in column flotation and its effect on recovery and grade. Canadian Metallurgical Quarterly, 51(2), 111–117. https://doi.org/10.1179/1879139511Y.0000000033
7. B. K. Gorain, J. P. Franzidis, E. V. Manlapig (2000). Flotation Cell Design: Application of Fundamental Principles, Julius Kruttschnitt Mineral Research Centre, Indooroopilly, Queensland, Australia, Academic Press.
8. Gembe Huaroco, J. E., Escudero García, R., & Arcos Gutiérrez, H. (2018). CFD simulation of a sparger type venturi to generate bubbles in a two-phase flotation system. 43(2), 263.
9. Huang, J., Sun, L. C., Du, M., Liang, Z., Mo, Z. Y., Tang, J. G., Xie, G. (2019). An investigation on the performance of a micro-scale Venturi bubble generator. Chemical Engineering Journal. https://doi.org/10.1016/j.cej.2019.02.068
10. Li Guiyi. (1992). Turbulence modelling. Proceedings - ICE: Water, Maritime & Energy, 96(3), 187–192. https://doi.org/10.1201/b19471-8
11. Xiangning Bu, Tuantuan Zhang, Yuran Chen, Guangyuan Xie & Yaoli Peng (2017): Comparative study of conventional cell and cyclonic microbubble flotation column for upgrading a difficult-to-float Chinese coking coal using statistical evaluation, International Journal of Coal Preparation and Utilization, DOI: 10.1080/19392699.2017.1359577
12. M. Wang, C. Ni, X. Bu, Y. Peng, G. Xie, Z. Tan, H. Yu, CFD-PBM simulation of the column flotation unit of FCMC: Importance of gas–liquid interphase forces models. The Canadian Journal of Chemical Engineering. 2023, 101(10), 5925. https://doi.org/10.1002/cjce.24828
13. Barigou, M., Greaves, M. (1991). A capillary suction probe for bubble size measurement. Meas. Sci. Technol., 2, 318–326.
14. Grau, R. A., Heiskanen, K. (2002). Visual technique for measuring bubble size in flotation machines. Minerals Engineering, 15(7), 507–513.
15. Escudero, R. (2007). Modelos matemáticos comúnmente empleados en sistemas de dispersión para estimar las características de las mismas, Programa de capacitación y adiestramiento SPUM, UMSNH.
16. Tavera, F. J., & Escudero García, R. (2013). Effect of Solids on Gas Holdup Characteristics in Flotation Column: Addition of Hydrophilic and Hydrophobic Solids. 56(2), 1–13.
17. Sarhan, A. R., Naser, J., & Brooks, G. (2016). CFD simulation on influence of suspended solid particles on bubbles' coalescence rate in flotation cell. International Journal of Mineral Processing, 146, 54–64. https://doi.org/10.1016/j.minpro.2015.11.014
18. Sarhan, A. R., Naser, J., & Brooks, G. (2017). CFD analysis of solid particles properties effect in three-phase flotation column. Separation and Purification Technology, 185, 1–9. https://doi.org/10.1016/j.seppur.2017.04.042
19. J.B. Yianatos, J.A. Finch, Gas holdup versus gas rate in the bubbly regime. International Journal of Mineral Processing, 29(1–2), 141–146 (1990). https://doi.org/10.1016/0301-7516(90)90011-M
20. Finch, J.A., Dobby, G.S. (1991). Column flotation: A selected review. Part I. International Journal of Mineral Processing, 33(1–4), 343–354. https://doi.org/10.1016/0301-7516(91)90062-N
21. Appendix 2 - List of ASTM International and AASHTO Test Methods Related to Asphalt Testing (Listed by Subject), Editor(s): James G. Speight, Asphalt Materials Science and Technology, Butterworth-Heinemann, 2016, Pages 531–562. https://doi.org/10.1016/B978-0-12-800273-5.00021-0
22. Reza M. Rahman, Seher Ata, Graeme J. Jameson (2012). The effect of flotation variables on the recovery of different particle size fractions in the froth and the pulp. International Journal of Mineral Processing, 106–109, 70–77. https://doi.org/10.1016/j.minpro.2012.03.001